HHS Public Access

Author manuscript

J Thorac Cardiovasc Surg. Author manuscript; available in PMC 2019 June 01.

Published in final edited form as:

J Thorac Cardiovasc Surg. 2018 June ; 155(6): 2277–2286.e2. doi:10.1016/j.jtcvs.2017.11.007.

Perioperative evaluation of regional aortic wall shear stress patterns in patients undergoing aortic valve and/or proximal thoracic aortic replacement

Emilie Bollache, PhD[1], **Paul WM Fedak, MD, PhD**[2,3], **Pim van Ooij, PhD**[4], **Ozair Rahman, MD**[1], **S Chris Malaisrie, MD**[3], **Patrick M McCarthy, MD**[3], **James C Carr, MD**[1], **Alex Powell, MS**[1], **Jeremy D Collins, MD**[1], **Michael Markl, PhD**[1,5], and **Alex J Barker, PhD**[1]

[1]Department of Radiology, Feinberg School of Medicine, Northwestern University, Chicago, IL USA [2]Department of Cardiac Sciences, Cumming School of Medicine, University of Calgary, Calgary, AB Canada [3]Division of Surgery-Cardiac Surgery, Northwestern University, Chicago, IL USA [4]Department of Radiology, Academic Medical Center, Amsterdam, the Netherlands [5]Department of Biomedical Engineering, McCormick School of Engineering, Northwestern University, Chicago, IL USA

Abstract

Objectives—To assess in patients with aortopathy perioperative changes in thoracic aortic wall shear stress (WSS), which is known to affect arterial remodeling, and the effects of specific surgical interventions.

Methods—Pre- and post-surgical aortic 4D flow MRI were performed in 33 aortopathy patients (54±14 years; 5 women; sinus of Valsalva (d_SOV)/mid-ascending aortic (d_MAA) diameters=44±5/45±6mm) scheduled for aortic valve (AVR) and/or root (ARR) replacement. Aortopathy control patients who did not have surgery were matched for age, sex, body size and d_MAA (n=20: 52±14 years; 3 women; d_SOV/d_MAA =42±4/42±4mm). Regional aortic 3D systolic peak WSS was calculated. Finally, an atlas of WSS normal values was used to quantify the percentage of 'at-risk' tissue area with abnormally high WSS, while excluding the area to be resected/graft.

Results—Peak WSS and at-risk area showed low inter-observer variability (≤0.09[−0.3;0.5]Pa and 1.1[−7;9]%, respectively). In control patients, WSS was stable over time (follow-up–baseline differences≤0.02Pa and 0.0%, respectively). Proximal aortic WSS decreased after AVR (n=5; peak WSS difference≤−0.41Pa and at-risk area≤−10%, $p<0.05$ vs. controls). WSS was increased after

Corresponding author: Alex J Barker, PhD, Northwestern University - 737 N Michigan ave Suite 1600 - Chicago, Illinois 60611, USA, Telephone: +1-312-926-2736/Fax: +1-312-926-5991, alex.barker@northwestern.edu.

IRB: #STU00202431 approved on 1/27/2016

Conflict of interest statement

See disclosure statements.

ARR in regions distal to the graft (peak WSS difference≥0.16Pa and at-risk area≥4%, p<0.05 vs. AVR). Follow-up duration had no significant effects on these WSS changes, except when comparing ascending aortic peak WSS between ARR and AVR (p=0.006).

Conclusions—Serial perioperative 4D flow MRI investigations revealed distinct patterns of post-surgical changes in aortic WSS which included both reductions and translocations. Larger longitudinal studies are warranted to validate these findings with clinical outcomes and prediction of risk of future aortic events.

Graphical Abstract

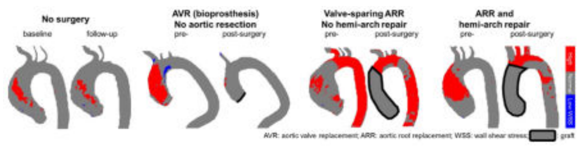

Keywords

wall shear stress; aortic valve replacement; aortic root replacement; hemi-arch repair; perioperative; 4D flow MRI

Introduction

Patients with thoracic aortic disease are often asymptomatic before acute critical events occur such as dissection or rupture. Early detection and management are necessary to minimize risk. When necessary, prophylactic surgical repair or replacement of the aorta and/or aortic valve is recommended. Currently, risk for these events is assessed from diameter measurements provided by either computed tomography, magnetic resonance imaging (MRI) or echocardiography(1). However, efforts to use advanced noninvasive imaging to risk-stratify these patients have been proposed(2). For example, the measurement of three-dimensional (3D) cine (time-resolved) blood flow with three-directional velocity encoding (known as ‘4D flow MRI’) has enabled the use of noninvasive MRI to investigate complex hemodynamics and 3D blood flow patterns.

Previous quantitative *in vivo* evaluations of post-operative aortic hemodynamics in the literature have mostly focused on transvalvular gradients(3–8), valvular regurgitation(3,4,9–11) or peak velocity(9,12,13). In addition, wall shear stress (WSS), defined as the tangential viscous force exerted by blood flow on the arterial wall, is an important potential biomarker, as it plays a major role in the regulation of cellular function and remodeling via endothelial mechanotransduction(14). For example, aortic WSS has been studied using 4D flow MRI after valve-sparing aortic root replacement (VS-ARR) in Marfan(15) or bicuspid aortic valve (BAV)(16) patients. It has also been used to compare different types of valve prosthesis after aortic valve replacement (AVR)(17) or in the evaluation of the impact of surgical and transcatheter AVR procedures(18). Importantly, a 4D flow MRI study in BAV patients has shown that aortic regions with abnormally increased WSS exhibited significant alterations of elastin fibers and extracellular matrix proteins implicated in aortic wall degeneration(19).

Studies have also investigated perioperative findings of aortic hemodynamics, but they primarily focused on valvular regurgitation(10,20), pressure gradient(7,10) or peak velocity(20), mainly in the setting of AVR. Of note, two studies have reported on WSS changes between pre-intervention and after surgical(21) or transcatheter(22) AVR, with a focus on investigating carotid and brachial WSS, respectively. However, to date, no comprehensive study has investigated pre- and post-operative aortic hemodynamic WSS data beyond that of aortic valve replacement alone. Thus, the purpose of this study is to compare pre- and post-surgical aortic WSS patterns in patients with aortopathy who underwent replacement of the aortic valve and/or the aorta, using 4D flow MRI. Follow-up 4D flow MRI data of patients with aortopathy who didn't have surgery were also investigated as controls. Our hypothesis is that surgery will impact on WSS, with different changes according to the performed intervention.

Materials and methods

Study population

All patients were identified, via Institutional Review Board-approved retrospective chart review with a waiver of consent, from a 1673 subjects 4D flow MRI database, i.e. phase-contrast MRI with velocity encoding in all three spatial directions that is resolved relative to all three dimensions of space (3D) and to the dimension of time (cine) along the cardiac cycle. We selected all patients with aortic and/or valve disease (n=1128). Among them, we included the n=244 who had undergone aortic valve and/or aorta replacement as well as post-operative clinically ordered standard of care cardiothoracic MRI, including 4D flow. We further identified patients who also had undergone a 4D flow exam before surgery (n=55). Finally, we excluded those with a history of aortic dissection or previous aortic interventions (n=21), as well as a single patient who underwent a modified Ross pulmonary autograft procedure, resulting in 33 patients and 66 MRI datasets. A consort flow diagram is provided in the Supplementary Figure. In addition, 20 “control” aortopathy patients matched for age, gender, height and weight, who underwent baseline and follow-up routine surveillance MRI (n=40 datasets) but no surgery in-between were included.

Surgical procedures

All operations were performed between 2012 and 2016.

VS-ARR was performed using a modified reimplantation technique, with a 34-mm Dacron graft. Coronary reconstruction was achieved with reimplantation of left and right coronary arteries as buttons, with a concomitant valve repair for all cases. A second smaller 24 to 28-mm graft was used to replace the tubular segment of the ascending aorta. Of note, a large, straight graft was used for the sinus portion.

Aortic root replacement (ARR) with concomitant AVR was performed using a modified Bentall procedure. The valve was sewn into a 7-mm larger Gelweave Dacron graft (VASCUTEK, Inchinnan, Scotland, UK). The annular sutures were passed through the valve conduit. The left main and right coronary ostia were anastomosed as buttons to the side of the conduit.

Further hemi-arch repair (HA), involving resection of the aorta up to its distal end from the base of the innominate artery to the lesser curve(23), was performed when the diameter of the proximal aortic arch was above 4cm.

In ARR combined with AVR as well as AVR alone procedures, different valve prostheses were used: bioprosthesis (23 to 29-mm Carpentier-Edwards pericardial PERIMOUNT or 23 to 27-mm Carpentier-Edwards pericardial Magna Ease or 27 to 29-mm Edwards INTUITY bovine pericardial valve; Edwards Lifesciences, Irvine, CA, USA) or a mechanical valve (23 to 27-mm On-X valve; CryoLife Inc, Kennesaw, GA, USA).

For each intervention, perfusion time, cross-clamp time and post-operative length of stay were recorded.

MRI acquisitions

All baseline and follow-up MRI exams were performed between 2011 and 2016.

Exam acquisition included ECG-gated 2D cine balanced steady state free precession images for the evaluation of cardiac volumes and function (left ventricular stroke volume [LVSV] and ejection fraction [LVEF]), as well as contrast-enhanced MR angiography (CE-MRA) of the thoracic aorta for aortic dimension characterization (sinuses of Valsalva [SOV] and mid-ascending aorta [AA] diameters). Furthermore, 2D cine through-plane phase-contrast MRI was performed at the aortic valve, for aortic valve disease evaluation (BAV morphology Sievers classification and severity of stenosis and regurgitation). Finally, an aortic 4D flow MRI was performed to subsequently derive peak velocity and wall shear stress. Details regarding MRI acquisition parameters and data analysis are provided in the Supplementary Material.

Quantification of baseline and follow-up aortic wall shear stress patterns from 4D flow MRI data

The analysis of each baseline and follow-up 4D flow MRI dataset, including preprocessing, calculation of a 3D angiogram and aortic segmentation, is illustrated in Figure 1.a and detailed in the Supplementary Material.

Maximum intensity projections (MIP) of the systolic absolute velocities inside the 3D segmentation were calculated and used to obtain the peak velocity (Vmax) in the vena contracta (Figure 1.b), using a previously described approach(24).

Finally, WSS, defined as the product between blood dynamic viscosity and the velocity spatial gradient at the wall, was calculated throughout the entire 3D aortic surface using an in-house Matlab algorithm(25). In particular, systolic WSS was averaged over 5 cardiac phases centered on the peak systolic phase, as defined by the time phase with the highest velocity averaged within the segmented aortic volume. Furthermore, aortic ‘heatmaps’ were created, using a healthy control atlas previously established in 56 controls representing the 95% confidence interval of the normal WSS range(26). For each patient and each baseline and follow-up 4D flow dataset, WSS 3D distribution was registered to this atlas, to identify regions with an abnormally elevated WSS, i.e. above the 95% confidence interval. Regional

WSS patterns were then characterized in the AA, the aortic arch and the proximal descending aorta (DA). The AA was defined by the region between the aortic valve and the first supra-aortic vessel, the aortic arch included the region between the first and last supra-aortic vessels and the proximal DA comprised the region from the last supra-aortic vessel takeoff to the corresponding level of the aortic valve. For each AA, arch and DA region (Figure 1.c): 1) peak WSS magnitude (averaged over the 2% highest values) and 2) 'at-risk' tissue area exposed to abnormally high WSS, calculated from the heatmap red regions and further expressed in percentage of the total area, were extracted. In surgery patients, both WSS indices were estimated while excluding the area to be resected and the graft, at pre-and post-surgery, respectively, as visually evaluated using CE-MRA or computed tomography angiography images when available. Thus, it was studied in the aortic arch and DA for all patients, and, in patients who underwent ARR, only in the ascending aortic region that was not replaced. In addition, total at-risk tissue absolute area in the whole aorta of no-surgery patients was also reported.

Inter-observer reproducibility

In order to assess their sensitivity to segmentation and their reproducibility, peak WSS magnitude and percentage at-risk tissue area were calculated from both baseline and follow-up datasets using aortic volume segmented by two blinded and independent operators in 10 randomized controls (including 5 patients with a tricuspid and 5 patients with a bicuspid aortic valve) and 10 randomized surgery patients (including 2 patients who underwent AVR alone, 5 patients who underwent ARR with no HA and 3 patients who underwent ARR and HA).

Statistical analysis

Normal distributions were tested using a Lilliefors test. Data are reported as mean ± standard deviation (SD) when their distribution was normal or otherwise as median (interquartile range). Follow-up duration and longitudinal changes in WSS indices were further studied in surgery subgroups according to the aortic valve type and performed intervention. Comparisons between patient groups were performed using a Wilcoxon rank-sum test, while differences between baseline and follow-up were tested using a Wilcoxon signed-rank test. We further investigated longitudinal WSS pattern changes as defined as follow-up minus baseline peak WSS and percentage at-risk tissue area differences. Differences in WSS change between patient groups were studied using linear mixed-effects models taking into account baseline WSS measurement, patient category (surgery vs. no surgery or intervention type), and follow-up duration. Finally, inter-observer variability was studied using Bland-Altman analyses and mean biases and limits of agreement (as defined as mean±1.96*SD) were provided. A value $p<0.05$ was considered as statistically significant. Statistical analyses were performed using Matlab (MathWorks, Natick, MA, USA).

Results

Patient baseline characteristics and surgery details

Patient baseline characteristics are summarized for the surgery and no-surgery groups in Table 1. SOV diameter was similar between the 2 patient groups, but, as expected, the mid-

AA was significantly more dilated in patients undergoing surgery. LVSV and LVEF were similar between the two groups. Finally, the median MRI follow-up duration was significantly longer for no-surgery (ranging from 1 to 4 years) than surgery patients (1 week to 3.3 years). Duration between baseline MRI and surgery ranged from 1 day to 3.3 years, while surgery to follow-up MRI duration ranged from 2 days and 2.6 years. At follow-up, changes in LVSV and LVEF were insignificant compared to baseline in both patient groups (91±29ml/92±21ml and 59±12%/58±8.7% in no-surgery/surgery patients, respectively; differences were insignificant between the 2 groups).

Subgrouping of surgery patients was further performed according to the intervention type and valve prosthesis, as shown in Table 2: 5 patients had AVR with no resection of the aorta. Among the remaining 28 patients who had ARR, 22 had concomitant AVR and 12 had further HA (ARR-HA$^+$). Median valve size was 27 (25–27)mm, maximum conduit size was 34 (34–34)mm, hemi-arch graft size was 26 (25–26)mm, perfusion time was 143±53min, cross-clamp time was 122±44min and post-operative length of stay was 5 (4–6)days. Follow-up surveillance time is further provided for each subgroup, revealing significantly longer durations for the AVR-alone group vs. all other surgery ARR patients with or without HA (p<0.01).

Longitudinal evolution of WSS patterns

Figures 2.a and 3.a illustrate baseline and follow-up aortic WSS magnitude MIP and heatmaps, respectively, in representative control and surgery patients by intervention and aortic valve type. The evolution over time of regional peak WSS and at-risk tissue percentage area is provided in Figures 2.b and 3.b, respectively.

In the no-surgery control group, the total absolute area of aortic at-risk tissue was 1.4 (0.4–5.4) and 1.7 (0.1–13)cm^2 at baseline and follow-up, respectively (p=0.57). In surgery patients, pre-intervention at-risk tissue area was 3.2 (0.0–36)cm^2 (non-significant vs. controls). After surgery, it was 7.8 (1.9–21)cm^2 (non-significant vs. pre-intervention area and vs. controls at follow-up). No significant regional differences between baseline and follow-up were observed for either aortic WSS index in both patient groups (Table 3), nor in surgery subgroups according to the intervention type. While both AA peak WSS and at-risk tissue area were similar between no-surgery and surgery patients at baseline, they were significantly higher in the latter group after intervention. We also observed increased WSS indices in surgery patients in the aortic arch at both baseline and follow-up, when compared to controls. Finally, DA peak WSS was significantly higher than controls in surgery patients at baseline, and was then normalized after intervention.

Quantitative differences between follow-up and baseline confirmed unchanged WSS indices in no-surgery patients (Figures 2.b and 3.b). It further revealed a significant decrease in AA and arch peak WSS in patients who underwent AVR alone when compared to changes in controls (p≤0.008), as well as a significant increase in ARR patients when compared to changes with AVR alone (p≤0.0008). Follow-up duration had no significant effects on these WSS changes, except when comparing the ARR-HA$^-$ and AVR groups in the AA (p=0.006). Similar tendencies were found for at-risk tissue area albeit restricted to the AA. Finally, no significant differences were observed between ARR-HA$^-$ and ARR-HA$^+$.

Inter-observer variability in WSS patterns evaluation

Inter-operator biases and limits of agreement for aortic WSS patterns assessed on the 40 datasets are provided in Table 4, indicating good reproducibility.

Discussion

Our main findings are: 1) peak WSS and at-risk tissue area decreased after surgery in patients who had AVR alone with a bioprosthesis; 2) WSS patterns were increased distal to the graft after ARR; 3) no significant difference in WSS changes was observed within the ARR group when HA was performed or not; 4) WSS indices showed high inter-observer reproducibility and remained consistent over time in patients without surgery.

Previous studies have described post-intervention aortic WSS in patients with aortic valve and/or aorta disease. One such study compared AVR with either a stented or stentless bioprosthesis, a mechanical valve, or autograft, against healthy controls(17). The authors reported a significant increase in peak systolic AA WSS in patients with bioprostheses when compared to autografts and controls. Of note, WSS values were higher in our study (mean value over the 4 patients with a stented bioprosthesis=1.8±0.3Pa; in the patient with a mechanical valve=1.4Pa) than theirs: stented bioprothesis=1.4±0.7Pa (n=14); mechanical valve~0.8Pa (n=9). This might be due to the fact that WSS was calculated in 2D planes orthogonal to the aorta while we used a 3D approach throughout the aortic wall, as well as the different follow-up duration after surgery (median value in our bioprosthesis group=380 (321–559)days vs. 3.6±2.6 years; in our mechanical valve patient=92 days vs. 7.9±3.6 years). Later, the same group investigated differences in WSS after transcatheter AVR (TAVI) compared to conventional surgical AVR, with a stented bioprosthesis, and healthy controls(18). The authors found that both AVR and TAVI groups had asymmetric WSS in the mid-AA with locally elevated and depressed WSS along circumference of the aorta, while it was uniform around the circumference in controls. We did not look at circumferential variations of WSS in the present study, but differences after surgery should be investigated in larger patient cohorts.

Another study investigated differences in aortic WSS in BAV patients with different leaflet fusion patterns after VS-ARR(16), resulting in eccentric WSS patterns with higher WSS on the outer curvature and lower WSS on the inner curvature. Finally, Hope et al. reported aortic WSS after VS-ARR in a specific population of patients with Marfan syndrome(15). They obtained variable changes in WSS depending on the aortic region (AA or DA) and local circumferential location (anterior right wall, inner or outer curvature), between patients and healthy volunteers, as well as in a patient who developed Stanford type B dissection during follow-up in which WSS patterns were altered.

All the aforementioned studies compared post-surgical findings with either healthy volunteers or pre-interventional findings obtained in different populations. To the best of our knowledge, only two studies reported same-patient pre- and post-surgical WSS values. However, these studies were investigating either the brachial(22) or carotid(21) arteries, both in the setting of atherosclerosis and not aortopathy, thus they focused on areas of pathologically low and oscillating WSS. In addition, both of these studies used ultrasound and a simple assumption of Poiseuille flow (based on single measurements of velocity and diameter) to calculate WSS(21,22). Given differences in vascular territories, methodological approaches and populations between these studies and ours, it is not possible to compare besides the finding that surgery altered the expression of WSS in the vessels investigated.

This work is a first effort to report same-patient pre- and post-surgical WSS patterns in the aorta, while pooling different types of interventions (AVR and/or ARR and/or HA). We combined non-invasive 4D flow MRI data with a three-dimensional method to compute WSS(25), which takes full advantage of the volumetric coverage of velocities at the wall when compared to approaches which are limited to 2D planes(27). This 3D WSS method was previously shown to provide good inter-observer and inter-scan reproducibility in healthy volunteers(28), which was confirmed by our low inter-observer variability obtained in patients including after surgery. Importantly, the inter-observer differences were lower compared to differences observed between pre- and post-surgery, indicating the potential of 4D flow-derived indices to reliably detect regions with altered wall shear forces.

It was previously shown that WSS was a key hemodynamic predictor of aneurysm dilatation(29). Until recently, aortic WSS could be assessed *in vivo* only using invasive techniques and was mostly estimated using computational fluid dynamics models(29–31). However, such models are limited by their underlying idealized assumptions on blood flow, arterial geometry and stiffness or boundary conditions, which are most of the time not patient-specific. In addition to systolic peak WSS magnitude, we studied the extent of 'at-risk' tissue exposed to an abnormally high WSS, as defined by the comparison to an atlas of normal WSS values. This 'heatmap' methodology allows to detect relative changes in WSS(26) and was recently demonstrated to correlate with resected tissue histology in BAV patients(19). More precisely, at-risk aortic regions of abnormally increased WSS exhibited significant reduction in elastin content, decreased elastin fiber thickness and increased fragmentation, when compared to regions with normal WSS in the same patient. At-risk tissue was further associated with significant changes in matrix metalloproteinase and transforming growth factor β-1 concentrations, indicating aortic wall extracellular matrix disruption. Given that the precise involvement of hemodynamics on aortopathy development is still unclear, we believe that the 4D flow MRI technique is a powerful and unique tool to investigate promising imaging biomarkers non-invasively(7,15,17,19,24–26,32,33). Importantly, the different changes observed within the surgery patients according to the intervention type suggest an opportunity to improve understanding the effects of different procedures and help surgeons deciding between AVR and/or ARR with or without HA, as well as what extent of aortic area should be resected. We speculate that the increase in peak WSS and at-risk tissue area distal to the graft after root surgery is due to the replacement of native elastic tissue by a stiff tube. Our results also suggest that resecting the aortic root vs. aortic valve replacement alone had more impact on WSS than further performing a hemiarch repair, in line with previous findings(23). Finally, the decrease in WSS patterns observed after biological AVR might be due to significantly longer follow-up in that group when compared to the remaining ARR patients, as suggested by the significant effect of follow-up duration on AA peak WSS change.

The main limitation of this pilot study is the small sample size. Indeed, care must be taken regarding statistical power when dividing surgery patients according to the performed intervention or replaced aortic valve. Furthermore, surgery subgroups were heterogeneous in terms of disease, resection extent, graft size, prosthesis type, or morphology of the native aortic valve. For instance, it would be interesting to investigate if WSS pattern changes are different between patients with either a native tricuspid, bicuspid or unicuspid aortic valve after VS-ARR, especially given the potential role of hemodynamics in mediating specifically BAV aortopathy. Finally, we lack outcome data and follow-up durations were variable among patients. However, follow-up duration was significantly shorter than controls for surgery patients in which we detected some changes in WSS patterns.

Future studies including more patients and longer follow-up at several systematic time points after surgery (1 month, 3 months, 6 months then yearly), as well as comparison to patient outcome, are warranted to help identifying robust indices able to refine the risk of future events, such as dilatation, rupture, subsequent aortic surgery or dissection, while optimizing the extent of aortic tissue to be resected(23). Finally, as our findings suggest an alteration of WSS patterns at the transition from graft to the native aorta, it might be complementary to investigate the effect of the stiff graft on downstream changes in hemodynamics(34).

Conclusion

Our study demonstrated the feasibility of 4D flow MRI to quantify pre- and post-surgical aortic WSS, resulting in different responses depending on the performed intervention. Future efforts are needed to investigate the ability of our WSS indices to predict disease progression and help guiding surgical resection as well as patient follow-up.

Supplementary Material

Refer to Web version on PubMed Central for supplementary material.

Acknowledgments

Sources of funding

This work was supported by the National Institutes of Health grants R01HL115828 and K25HL119608 as well as the American Heart Association Midwest Affiliate grant 16POST27250158.

Glossary of Abbreviations

4D flow MRI	three-dimensional time-resolved PC-MRI with three-directional velocity encoding
AA	ascending aorta
ARR	aortic root replacement
AVR	aortic valve replacement
BAV	bicuspid aortic valve

CE-MRA	contrast-enhanced magnetic resonance angiography
DA	descending aorta
EDV	end-diastolic volume
ESV	end-systolic volume
HA	hemi-arch repair
LV	left ventricle
LVEF	left ventricular ejection fraction
LVSV	left ventricular stroke volume
MAA	mid-AA
MIP	maximum intensity projection
MRI	magnetic resonance imaging
Pa	Pascal
PC	phase-contrast
SD	standard deviation
SOV	sinus of Valsalva
TAVI	transcatheter AVR
Vmax	peak velocity
VS-ARR	valve-sparing ARR
WSS	wall shear stress

References

1. Hiratzka LF, Bakris GL, Beckman JA, Bersin RM, Carr VF, Casey DE Jr, et al. 2010 ACCF/AHA/AATS/ACR/ASA/SCA/SCAI/SIR/STS/SVM Guidelines for the diagnosis and management of patients with thoracic aortic disease. A Report of the American College of Cardiology Foundation/American Heart Association Task Force on Practice Guidelines, American Association for Thoracic Surgery, American College of Radiology, American Stroke Association, Society of Cardiovascular Anesthesiologists, Society for Cardiovascular Angiography and Interventions, Society of Interventional Radiology, Society of Thoracic Surgeons, and Society for Vascular Medicine. J Am Coll Cardiol. 2010; 55:e27–e129. [PubMed: 20359588]
2. Della Corte A, Body SC, Booher AM, Schaefers HJ, Milewski RK, Michelena HI, et al. Surgical treatment of bicuspid aortic valve disease: knowledge gaps and research perspectives. J Thorac Cardiovasc Surg. 2014; 147:1749–57. 57 e1. [PubMed: 24534676]
3. Melina G, De Robertis F, Gaer JA, Amrani M, Khaghani A, Yacoub MH. Mid-term pattern of survival, hemodynamic performance and rate of complications after medtronic freestyle versus homograft full aortic root replacement: results from a prospective randomized trial. J Heart Valve Dis. 2004; 13:972–5. discussion 5–6. [PubMed: 15597592]

4. Fairbairn TA, Steadman CD, Mather AN, Motwani M, Blackman DJ, Plein S, et al. Assessment of valve haemodynamics, reverse ventricular remodelling and myocardial fibrosis following transcatheter aortic valve implantation compared to surgical aortic valve replacement: a cardiovascular magnetic resonance study. Heart. 2013; 99:1185–91. [PubMed: 23749779]
5. Amat-Santos IJ, Dahou A, Webb J, Dvir D, Dumesnil JG, Allende R, et al. Comparison of hemodynamic performance of the balloon-expandable SAPIEN 3 versus SAPIEN XT transcatheter valve. Am J Cardiol. 2014; 114:1075–82. [PubMed: 25132330]
6. Sharma V, Deo SV, Altarabsheh SE, Cho YH, Erwin PJ, Park SJ. Comparison of the early haemodynamics of stented pericardial and porcine aortic valves. Eur J Cardiothorac Surg. 2015; 47:4–10. [PubMed: 25123674]
7. Keller EJ, Malaisrie SC, Kruse J, McCarthy PM, Carr JC, Markl M, et al. Reduction of aberrant aortic haemodynamics following aortic root replacement with a mechanical valved conduit. Interact Cardiovasc Thorac Surg. 2016; 23:416–23. [PubMed: 27245620]
8. Oechtering TH, Hons CF, Sieren M, Hunold P, Hennemuth A, Huellebrand M, et al. Time-resolved 3-dimensional magnetic resonance phase contrast imaging (4D Flow MRI) analysis of hemodynamics in valve-sparing aortic root repair with an anatomically shaped sinus prosthesis. J Thorac Cardiovasc Surg. 2016; 152:418–27e1. [PubMed: 27423836]
9. Botnar R, Nagel E, Scheidegger MB, Pedersen EM, Hess O, Boesiger P. Assessment of prosthetic aortic valve performance by magnetic resonance velocity imaging. MAGMA. 2000; 10:18–26. [PubMed: 10697222]
10. Watanabe Y, Chevalier B, Hayashida K, Leong T, Bouvier E, Arai T, et al. Comparison of multislice computed tomography findings between bicuspid and tricuspid aortic valves before and after transcatheter aortic valve implantation. Catheter Cardiovasc Interv. 2015; 86:323–30. [PubMed: 25594190]
11. Salaun E, Jacquier A, Theron A, Giorgi R, Lambert M, Jaussaud N, et al. Value of CMR in quantification of paravalvular aortic regurgitation after TAVI. Eur Heart J Cardiovasc Imaging. 2016; 17:41–50. [PubMed: 26188194]
12. Torii R, El-Hamamsy I, Donya M, Babu-Narayan SV, Ibrahim M, Kilner PJ, et al. Integrated morphologic and functional assessment of the aortic root after different tissue valve root replacement procedures. J Thorac Cardiovasc Surg. 2012; 143:1422–8. [PubMed: 22361248]
13. Kidher E, Cheng Z, Jarral OA, O'Regan DP, Xu XY, Athanasiou T. In-vivo assessment of the morphology and hemodynamic functions of the BioValsalva composite valve-conduit graft using cardiac magnetic resonance imaging and computational modelling technology. J Cardiothorac Surg. 2014; 9:193. [PubMed: 25488105]
14. Tanweer O, Wilson TA, Metaxa E, Riina HA, Meng H. A comparative review of the hemodynamics and pathogenesis of cerebral and abdominal aortic aneurysms: lessons to learn from each other. J Cerebrovasc Endovasc Neurosurg. 2014; 16:335–49. [PubMed: 25599042]
15. Hope TA, Kvitting JP, Hope MD, Miller DC, Markl M, Herfkens RJ. Evaluation of Marfan patients status post valve-sparing aortic root replacement with 4D flow. Magn Reson Imaging. 2013; 31:1479–84. [PubMed: 23706513]
16. Stephens EH, Hope TA, Kari FA, Kvitting JP, Liang DH, Herfkens RJ, et al. Greater asymmetric wall shear stress in Sievers' type 1/LR compared with 0/LAT bicuspid aortic valves after valve-sparing aortic root replacement. J Thorac Cardiovasc Surg. 2015; 150:59–68. [PubMed: 25956338]
17. von Knobelsdorff-Brenkenhoff F, Trauzeddel RF, Barker AJ, Gruettner H, Markl M, Schulz-Menger J. Blood flow characteristics in the ascending aorta after aortic valve replacement--a pilot study using 4D-flow MRI. Int J Cardiol. 2014; 170:426–33. [PubMed: 24315151]
18. Trauzeddel RF, Lobe U, Barker AJ, Gelsinger C, Butter C, Markl M, et al. Blood flow characteristics in the ascending aorta after TAVI compared to surgical aortic valve replacement. Int J Cardiovasc Imaging. 2016; 32:461–7. [PubMed: 26493195]
19. Guzzardi DG, Barker AJ, van Ooij P, Malaisrie SC, Puthumana JJ, Belke DD, et al. Valve-Related Hemodynamics Mediate Human Bicuspid Aortopathy: Insights From Wall Shear Stress Mapping. J Am Coll Cardiol. 2015; 66:892–900. [PubMed: 26293758]
20. Crouch G, Bennetts J, Sinhal A, Tully PJ, Leong DP, Bradbrook C, et al. Early effects of transcatheter aortic valve implantation and aortic valve replacement on myocardial function and

aortic valve hemodynamics: insights from cardiovascular magnetic resonance imaging. J Thorac Cardiovasc Surg. 2015; 149:462–70. [PubMed: 25455463]

21. Irace C, Gnasso A, Cirillo F, Leonardo G, Ciamei M, Crivaro A, et al. Arterial remodeling of the common carotid artery after aortic valve replacement in patients with aortic stenosis. Stroke. 2002; 33:2446–50. [PubMed: 12364736]
22. Horn P, Stern D, Veulemans V, Heiss C, Zeus T, Merx MW, et al. Improved endothelial function and decreased levels of endothelium-derived microparticles after transcatheter aortic valve implantation. Euro Intervention. 2015; 10:1456–63. [PubMed: 25287265]
23. Malaisrie SC, Duncan BF, Mehta CK, Badiwala MV, Rinewalt D, Kruse J, et al. The addition of hemiarch replacement to aortic root surgery does not affect safety. J Thorac Cardiovasc Surg. 2015; 150:118–24e2. [PubMed: 25896462]
24. Rose MJ, Jarvis K, Chowdhary V, Barker AJ, Allen BD, Robinson JD, et al. Efficient method for volumetric assessment of peak blood flow velocity using 4D flow MRI. J Magn Reson Imaging. 2016; 44:1673–82. [PubMed: 27192153]
25. Potters WV, van Ooij P, Marquering H, vanBavel E, Nederveen AJ. Volumetric arterial wall shear stress calculation based on cine phase contrast MRI. J Magn Reson Imaging. 2015; 41:505–16. [PubMed: 24436246]
26. van Ooij P, Potters WV, Nederveen AJ, Allen BD, Collins J, Carr J, et al. A methodology to detect abnormal relative wall shear stress on the full surface of the thoracic aorta using four-dimensional flow MRI. Magn Reson Med. 2015; 73:1216–27. [PubMed: 24753241]
27. Stalder AF, Russe MF, Frydrychowicz A, Bock J, Hennig J, Markl M. Quantitative 2D and 3D phase contrast MRI: optimized analysis of blood flow and vessel wall parameters. Magn Reson Med. 2008; 60:1218–31. [PubMed: 18956416]
28. van Ooij P, Powell AL, Potters WV, Carr JC, Markl M, Barker AJ. Reproducibility and interobserver variability of systolic blood flow velocity and 3D wall shear stress derived from 4D flow MRI in the healthy aorta. J Magn Reson Imaging. 2016; 43:236–48. [PubMed: 26140480]
29. Pasta S, Rinaudo A, Luca A, Pilato M, Scardulla C, Gleason TG, et al. Difference in hemodynamic and wall stress of ascending thoracic aortic aneurysms with bicuspid and tricuspid aortic valve. J Biomech. 2013; 46:1729–38. [PubMed: 23664314]
30. Arzani A, Suh GY, Dalman RL, Shadden SC. A longitudinal comparison of hemodynamics and intraluminal thrombus deposition in abdominal aortic aneurysms. Am J Physiol Heart Circ Physiol. 2014; 307:H1786–95. [PubMed: 25326533]
31. Lei M, Archie JP, Kleinstreuer C. Computational design of a bypass graft that minimizes wall shear stress gradients in the region of the distal anastomosis. J Vasc Surg. 1997; 25:637–46. [PubMed: 9129618]
32. Bogren HG, Buonocore MH, Follette DM. Four-dimensional aortic blood flow patterns in thoracic aortic grafts. J Cardiovasc Magn Reson. 2000; 2:201–8. [PubMed: 11545117]
33. Kvitting JP, Ebbers T, Wigstrom L, Engvall J, Olin CL, Bolger AF. Flow patterns in the aortic root and the aorta studied with time-resolved, 3-dimensional, phase-contrast magnetic resonance imaging: implications for aortic valve-sparing surgery. J Thorac Cardiovasc Surg. 2004; 127:1602–7. [PubMed: 15173713]
34. Aquaro GD, Briatico Vangosa A, Toia P, Barison A, Ait-Ali L, Midiri M, et al. Aortic elasticity indices by magnetic resonance predict progression of ascending aorta dilation. Eur Radiol. 2016

Central message

Differing proximal aorta interventions induced distinct changes in wall shear stress (WSS). Further research is needed to validate 4D flow MRI WSS to predict outcome and inform surgical practice.

Perspective statement

Changes in pre- and post-surgical aortic wall shear stress in the face of different interventions (valve and/or root replacement with or without hemiarch repair) are reported herein for the first time. Given the potential role of hemodynamics on the progression of aortopathy, this non-invasive imaging biomarker may identify patients at high risk for future events and optimize operative strategies.

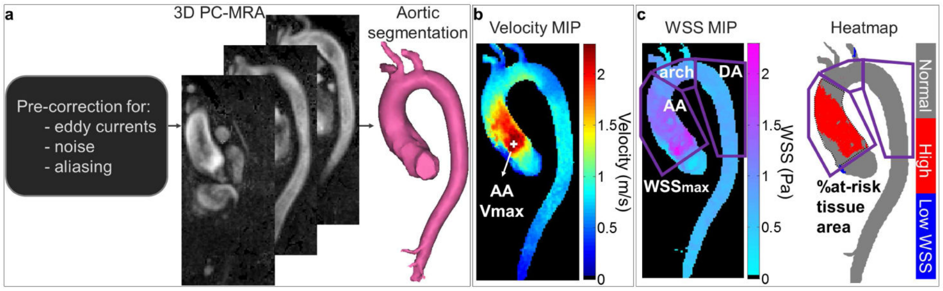

Figure 1.

Analysis of aortic 4D flow MRI data. a) Preprocessing, calculation of the 3D phase-contrast angiogram (PC-MRA) and segmentation of the aortic volume. b) Estimation of systolic peak velocity (Vmax, location indicated by the white marker) in the vena contracta, from velocity maximal intensity projections (MIP). c) Evaluation of wall shear stress (WSS) patterns along the AA, arch and descending aorta (DA) wall (purple regions of interest): 1) systolic peak magnitude (WSSmax) provided by the WSS MIP; 2) at-risk tissue percentage area, defined as regions with a WSS above normal values (mean+1.96xstandard deviation of WSS atlas values averaged over a group of 56 healthy volunteers) provided by the heatmap (in red). The dotted line on the heatmap indicates the area to be resected.

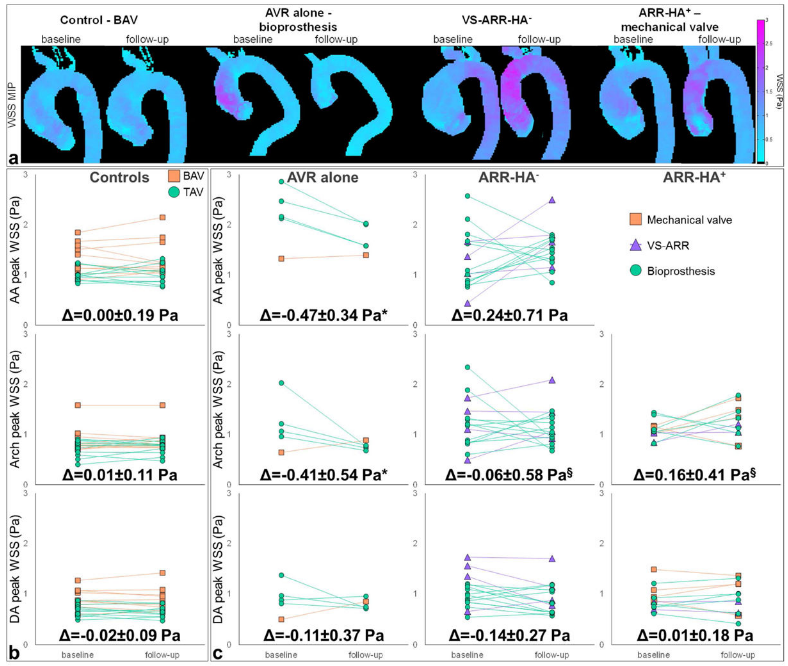

Figure 2.

a. Baseline and follow-up aortic WSS magnitude MIP in representative control and surgery patients who underwent different intervention and aortic valve types, from left to right: BAV control, aortic valve replacement (AVR) alone with a bioprosthesis, valve-sparing aortic root replacement with no hemi-arch repair (VS-ARR-HA$^-$) and ARR with hemi-arch repair (ARR-HA$^+$) with a mechanical valve. b. Evolution of peak WSS magnitude from baseline to follow-up in the control and c. the surgery groups according to aortic valve type (see legends). The surgery group was further divided according to the performed intervention, from left to right: AVR alone, ARR-HA− and ARR-HA+. Longitudinal changes (Δ), as defined by follow-up – baseline differences, are provided for each patient group and aortic region: ascending aorta (AA, top row), aortic arch (middle row) and descending aorta (DA, bottom row). Of note, results were not reported in the AA for the ARR-HA+ group because the entire region was resected during surgery. *: $p<0.05$ against control group, §: $p<0.05$ against AVR group, with non-significant effects of follow-up duration.

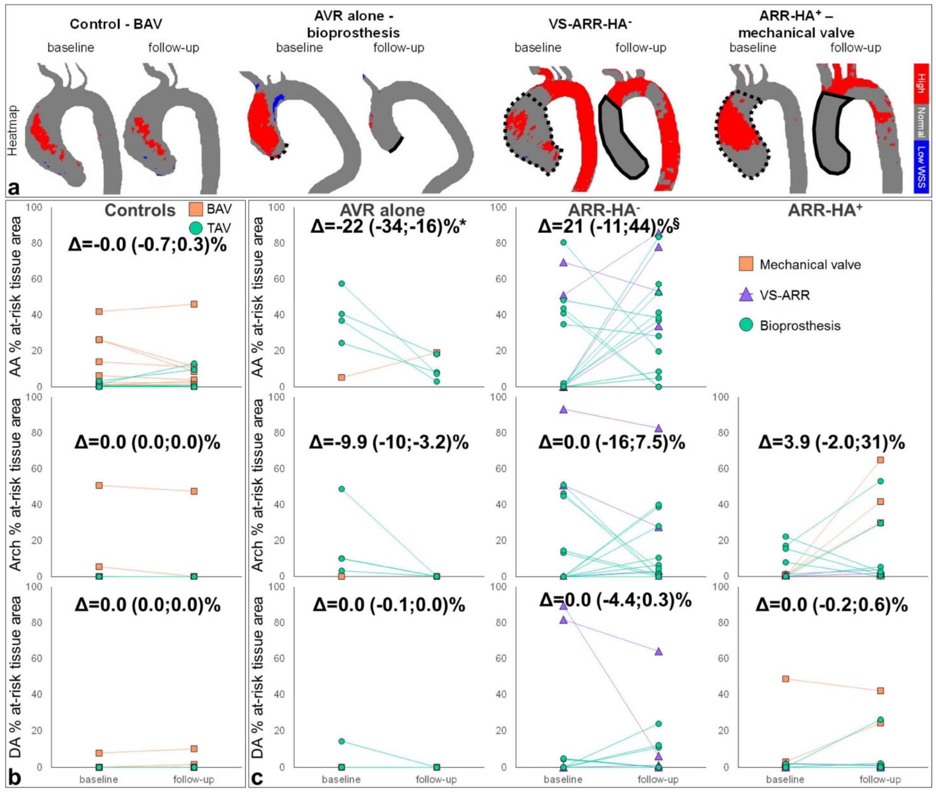

Figure 3.

a. Baseline and follow-up aortic WSS heatmap in representative control and surgery patients who underwent different intervention and aortic valve types, from left to right: BAV control, aortic valve replacement (AVR) alone with a bioprosthesis, valve-sparing aortic root replacement with no hemi-arch repair (VS-ARR-HA−) and ARR with hemi-arch repair (ARR-HA+) with a mechanical valve. In surgery patient heatmaps, dotted lines indicate the area to be resected and solid lines indicate the position of the graft at baseline and follow-up, respectively. b. Evolution of percentage at-risk tissue area from baseline to follow-up in the control and c. the surgery groups according to aortic valve type (see legends). The surgery group was further divided according to the performed intervention, from left to right: AVR alone, ARR-HA$^-$ and ARR-HA$^+$. Longitudinal changes (Δ), as defined by follow-up – baseline differences, are provided for each patient group and aortic region: AA (top row), aortic arch (middle row) and DA (bottom row). Of note, results were not reported in the AA for the ARR-HA$^+$ group because the entire region was resected during surgery. *: $p<0.05$ against control group, §: $p<0.05$ against AVR group, with non-significant effects of follow-up duration.

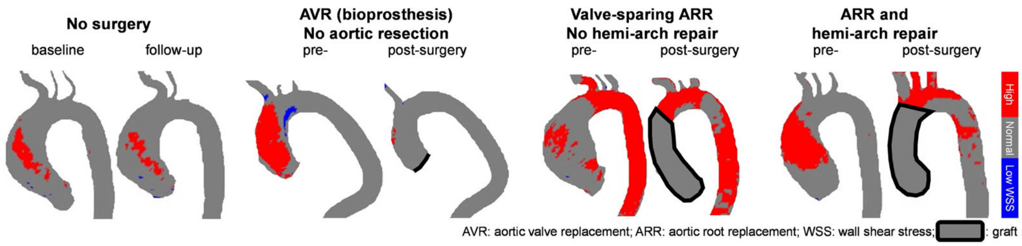

Central picture.

Changes in "at-risk" tissue (red) for control (no surgery) and aortic surgery patients.

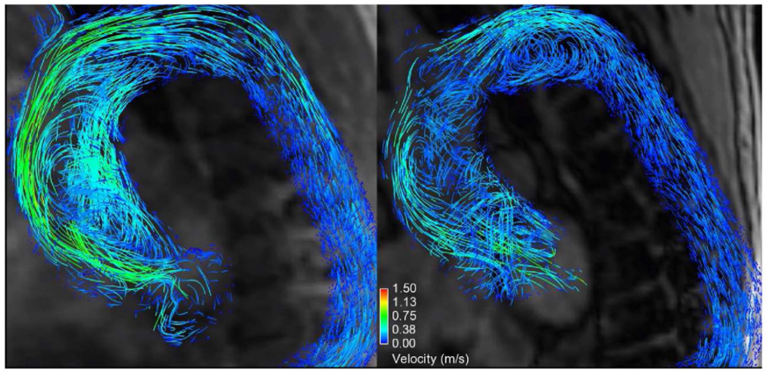

Video.

Comparison of blood flow patterns in the proximal aorta provided by 4D flow MRI at pre- and post-surgery (left and right, respectively), in a 71-year-old man with BAV. The patient underwent AVR with a 27-mm Edwards INTUITY bovine pericardial valve for moderate to severe aortic valve stenosis and mild insufficiency. In this case, blood flow was altered with reduced velocities and shear stress at the wall, suggesting blood flow pattern normalization after AVR.

Table 1

Baseline characteristics, aortic valve and left ventricular function and aortic diameters, as well as follow-up durations according to patient group.

	No surgery (n=20)	Surgery (n=33)
Women	n=3 (15%)	n=5 (15%)
Age	52±14 years	54±14 years
Height	178±9.4 cm	175±10 cm
Weight	89±15 kg	87±15 kg
BAV	n=10 (50%)	n=25 (76%)
type 0		
ap	N=1	n=3
lat	N=2	n=2
type 1		
LR	N=5	n=12
RN	N=1	n=4
type 2 - LR/RN	N=1	n=4
AS: none/trace/mild/moderate/severe	19/0/1/0/0	16/7/2/6/2
AI: none/trace/mild/moderate/severe	5/5/8/2/0	5/7/12/6/3
SOV diameter	41.8±4.1 mm	44.0±5.2 mm
Mid-AA diameter	41.8±4.0 mm	45.2±6.3 mm *
SBP/DBP	128±13/77±8.9 mmHg	128±16/77±13 mmHg
LV SV	85±22 ml	105±36 ml
LV EF	62±7.2%	60±8.6%
Heart rate	65±8.6 bpm	69±14 bpm
MRI follow-up duration	854 (419–1067) days	48 (26–191) days *
baseline MRI to surgery	-	21 (15–49) days
surgery to follow-up MRI	-	6 (4–20) days

BAV: bicuspid aortic valve; AS: aortic stenosis; AI: aortic insufficiency; SOV: sinus of Valsalva; AA: ascending aorta; SBP/DBP: systolic/diastolic blood pressures; LV: left ventricular; SV: left ventricular stroke volume; EF: ejection fraction.

* $p<0.05$ between surgery and no-surgery groups.

Table 2

Summary of performed interventions and replaced aortic valve types in the surgery group. Baseline to follow-up MRI duration as well as surgery to follow-up MRI duration (in days) are provided for each subgroup.

	AVR alone (n=5)	**ARR-HA $^-$ (n=16)**	**ARR-HA $^+$ (n=12)**
Bioprosthesis	**n=4**	**n=12**	**n=6**
MRI f-u duration	*408 (334–594) days*	*43 (27–102) days*	*32 (20–40) days*
surgery to f-u MRI	*380 (321–559) days*	*6 (5–18) days*	*6 (5–17) days*
Mechanical valve	**n=1**	**n=0**	**n=4**
MRI f-u duration	*141 days*	-	*56 (33–72) days*
surgery to f-u MRI	*92 days*	-	*4 (3–5) days*
VS-ARR		**n=4**	**n=2**
MRI f-u duration	-	*33 (20–45) days*	*191;1200 days*
surgery to f-u MRI		*4 (3–9) days*	*6;3 days*

AVR: aortic valve replacement; ARR-HA$^-$: aortic root replacement with no hemi-arch repair; ARR-HA$^+$: aortic root replacement and hemi-arch repair; f-u: follow-up; VS-ARR: valve-sparing ARR

Table 3

Peak velocity in the vena contracta, as well as peak WSS and percentage at-risk tissue area in the AA, aortic arch and DA at baseline and follow-up according to patient group.

	No surgery (n=20)		Surgery (n=33)	
	baseline	***follow-up***	***baseline***	***follow-up***
Vmax (m/s)	1.88±0.63	1.94±0.64	2.95±1.20 *	2.50±0.46 *
Peak WSS (Pa)				
AA	1.17±0.29	1.17±0.34	1.50±0.68	1.57±0.37 *
Arch	0.81±0.24	0.82±0.22	1.16±0.40 *	1.13±0.35 *
DA	0.79±0.20	0.77±0.22	0.97±0.29 *	0.89±0.28
At-risk tissue area (%)				
AA	1.0 (0.3–4.0)	1.1 (0.1–8.8)	24 (0.2–44)	28 (8.2–52) *
Arch	0 (0–0)	0 (0–0)	1.1 (0–15) *	2.6 (0–28) *
DA	0 (0–0)	0 (0–0)	0 (0–2.1)	0 (0–2.2)

Vmax: peak velocity; WSS: w all shear stress; AA: ascending aorta; DA: descending aorta.

* p<0.05 between surgery and no-surgery groups seperately at baseline and follow-up.

Table 4

Biases [limits of agreement] for the inter-operator variability of regional aortic WSS indices at baseline and follow-up in each patient group.

	No surgery (n=10)		Surgery (n=10)	
	baseline	***follow-up***	***baseline***	***follow-up***
Peak WSS (Pa)				
AA	0.05 [−0.12;0.22]	−0.05 [−0.25;0.14]	0.08 [−0.21;0.36]	0.09 [−0.27;0.45]
Arch	0.01 [−0.03;0.04]	0.00 [−0.03;0.04]	0.01 [−0.07;0.09]	0.02 [−0.08;0.11]
DA	0.00 [−0.04;0.04]	−0.00 [−0.02;0.01]	−0.00 [−0.04;0.04]	−0.00 [−0.03;0.02]
At-risk tissue area s(%)				
AA	0.4 [−1.1;1.9]	0.2 [−3.2;3.6]	−0.1 [−5.8;5.5]	−1.1 [−9.4;7.2]
Arch	0.8 [−4.0;5.6]	0.1 [−0.3;0.4]	0.8 [−5.4;7.0]	0.8 [−3.4;5.1]
DA	−0.0 [−0.2;0.2]	−0.1 [−1.2;1.0]	0.1 [−1.9;2.0]	−0.0 [−0.4;0.3]

WSS: w all shear stress; AA: ascending aorta; DA: descending aorta.